

DNA Binding of an Ethidium Intercalator Attached to a Monolayer-Protected Gold Cluster

Gangli Wang, Jian Zhang, and Royce W. Murray*

Kenan Laboratories of Chemistry, University of North Carolina, Chapel Hill, North Carolina 27599

Ethidium intercalation has been investigated as a means of inducing binding of Au nanoparticles to DNA. The ethidium sites are attached to the nanoparticles as thiolate ligands, using 3,8-diamino-5-mercaptododecyl-6-phenylphenanthridinium (ethidium thiolate). Each nanoparticle bears only one or two ethidium thiolate ligands. The rest of the thiolate monolayer ligands on the monolayer-protected Au clusters (MPCs) were either *N*-(2-mercaptopropionyl)glycine (tiopronin/ethidium MPC) or trimethyl-(mercaptoundecyl)ammonium (TMA/ethidium MPC). In solution mixtures of DNA and MPCs, the energy-transfer quenching of the ethidium ligands by the metal-like MPC core is partially released by ethidium binding to DNA, as observed by an increase in the intensity of ethidium fluorescence. Binding of the cationic TMA/ethidium MPC to DNA was efficient and rapid. The negatively charged tiopronin/ethidium MPC, in contrast, exhibits slow intercalation kinetics, relative to ethidium cation not attached to an MPC. The slow kinetics were analyzed as two competing binding interactions. The tiopronin/ethidium MPC binding to DNA was imaged by AFM.

The chemistry of nanoparticles¹ is a subject of much current interest. Over the past several years our laboratory has developed^{2–9} the chemistry of monolayer-protected Au clusters (MPCs). The initially reported MPCs, starting with those described by Brust et al.,¹⁰ had hydrophobic monolayers and were not water-soluble.

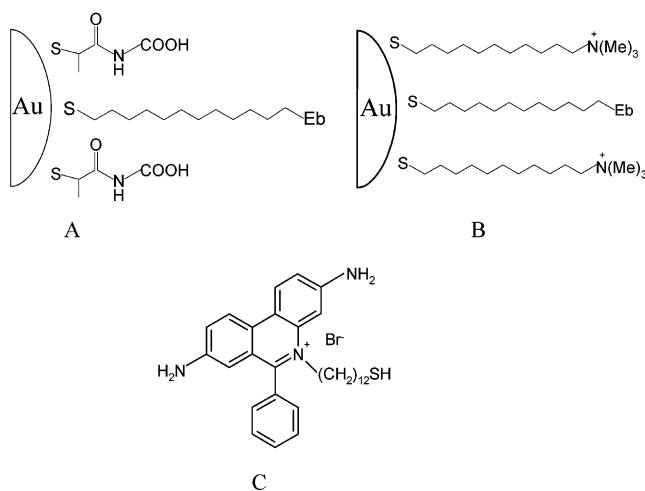


Figure 1. Cartoon of mixed monolayers (A) of tiopronin and ethidium thiolate (Eb) and (B) of TMA and Eb, and (C) structure of ethidium thiol.

We subsequently described^{5,6} the synthesis of water-soluble MPCs having tiopronin thiolate monolayers (tiopronin MPCs, tiopronin is *N*-(2-mercaptopropionyl)glycine) and their luminescence⁷ and the synthesis⁸ of water-soluble MPCs having *N,N,N*-trimethyl-(mercaptoundecyl)ammonium¹¹ (TMA MPCs) thiolate ligands. The monolayers of these and other MPCs can be converted into mixed monolayers by ligand place exchange^{2,6,9,12} reactions.

In this paper, we use place exchange to insert one or two ethidium thiolate ligands into the monolayers of water-soluble MPCs to prepare tiopronin/ethidium MPCs and TMA/ethidium MPCs. The average core sizes of these MPCs are 1.8 ± 0.7 and 4.4 ± 1.6 nm.^{5,8} The ethidium derivative employed, 3,8-diamino-5-mercaptododecyl-6-phenylphenanthridinium bromide (ethidium thiol), was prepared by a pathway analogous to a previous¹³ ethidium study. The structure of ethidium thiol and cartoons of its mixed monolayers with tiopronin and TMA thiolates are shown in Figure 1. The design of mixed-monolayer MPCs aims at using ethidium thiolate ligands to induce intercalation-based binding of the MPC nanoparticles to DNA in solutions of the two. The place

* Author to whom correspondence should be addressed. E-mail: rwm@email.unc.edu.

- (1) Schmid, G. *Clusters and Colloids. From Theory to Applications*; VCH: New York, 1994.
- (2) Ingram, R. S.; Hostetler, M. J.; Murray, R. W.; Schaaff, T. G.; Khoury, J. T.; Whetten, R. L.; Bigioni, T. P.; Guthrie, D. K.; First, P. N. *J. Am. Chem. Soc.* **1997**, *119*, 9279.
- (3) Hostetler, M. J.; Wingate, J. E.; Zhong, C.; Harris, J. E.; Vachet, R. W.; Clark, M. R.; Londono, J. D.; Green, S. J.; Stokes, J. J.; Wignall, G. D.; Glush, G. L.; Porter, M. D.; Evans, D.; Murray, R. W. *Langmuir* **1998**, *14*, 17.
- (4) Chen, S.; Ingram, R. S.; Hostetler, M. J.; Pietron, J. J.; Murray, R. W.; Schaaf, T. G.; Khoury, J. T.; Alvarez, M. M.; Whetten, R. L. *Science* **1998**, *280*, 2098.
- (5) Templeton, A. C.; Chen, S.; Gross, S. M.; Murray, R. W. *Langmuir* **1999**, *15*, 66.
- (6) Templeton, A. C.; Cliffl, D. E.; Murray, R. W. *J. Am. Chem. Soc.* **1999**, *121*, 7081.
- (7) Huang, T.; Murray, R. W. *J. Phys. Chem. B* **2001**, *105*, 1249.
- (8) Cliffl, D. E.; Zamborini, F. P.; Gross, S. M.; Murray, R. W. *Langmuir* **2000**, *16*, 9699.
- (9) Templeton, A. C.; Wuelfing, W. P.; Murray, R. W. *Acc. Chem. Res.* **2000**, *33*, 77.

- (10) Brust, M.; Walker, M.; Bethell, D.; Schiffrin, D. J.; Whyman, R. *J. Chem. Soc., Chem. Commun.* **1994**, 801.
- (11) Tien, J.; Terfort, A.; Whitesides, G. M. *Langmuir* **1997**, *13*, 5349.
- (12) (a) Hostetler, M. J.; Green, S. J.; Stokes, J. J.; Murray, R. W. *J. Am. Chem. Soc.* **1996**, *118*, 4212. (b) Green, S. J.; Stokes, J. J.; Hostetler, M. J.; Pietron, J. J.; Murray, R. W. *J. Phys. Chem. B* **1997**, *101*, 2663.
- (13) Ross, S. A.; Pittié, M.; Meunier, B. *J. Chem. Soc., Perkin Trans. 1* **2000**, 571.

exchange reaction was adjusted to incorporate only one or two ethidium sites into the mixed monolayer, avoiding the complexity of multiple binding events and DNA cross-linking.

A number of previous studies have reported nanoparticle–DNA binding based on sequence-specific molecular recognition properties to connect DNA oligonucleotides to nanoparticles. Mirkin et al.¹⁴ used thiol-modified noncomplementary DNA oligonucleotides to assemble gold nanoparticles (core sizes of >10 nm) into macroscopic aggregates whose formation was signaled by optical changes. Alivisatos et al.¹⁵ used an analogous approach to fashion two- or three-dimensional assemblies of nanoparticles. Electrostatic binding of a cationic TMA MPC was used by Rotello et al.¹⁶ in a study of the inhibition of DNA transcription. This paper presents the first example of using a known intercalator, ethidium, to induce nanoparticle–DNA binding.

It is well known that weak noncovalent bonds play crucial roles in interactions in biological structures.¹⁷ There is an extensive literature on interactions between DNA and molecular and metal complex probes, within which three modes of association are generally distinguished:¹⁸ external binding, groove binding, and intercalation. Intercalation refers to insertion of a molecular probe, which is usually a polyaromatic heterocyclic like proflavine or ethidium, between DNA base pairs.¹⁹ The ethidium cation is a well-known intercalator²⁰ that displays a large fluorescence enhancement (~25-fold) upon binding. Ethidium and its derivatives are widely used to study interactions with nucleic acids.²¹ Because DNA is a complex reactant and the ethidium interaction with it is kinetically quite fast,²² there has been uncertainty about some details of the reaction, with claims of single- and of multiple-step reactions, and of a diffusion-controlled rate and of an activated process. Some of the differences might be ascribed to different reaction conditions (concentration, buffer solution) used in the investigation. The study by Meyer-Almes and Porschke²³ using temperature-jump relaxation and stopped-flow measurements seems especially thorough. Their results were interpreted in terms of an activated reaction involving dual, interconvertible binding sites resulting from major and minor groove intercalation.

In the present study, we find that incorporating the ethidium thiol into the MPC monolayer results in a strong quenching of its fluorescence, presumably by energy-transfer interactions with the metal-like Au core of the nanoparticle. Such energy-transfer quenching by MPCs has been previously observed.²⁴ When the tiopronin/ethidium or TMA/ethidium MPC is mixed with DNA, a substantial increase in ethidium fluorescence is observed. We interpret this as intercalation-induced nanoparticle–DNA binding. Binding of the cationic TMA/ethidium MPC to the polyanionic DNA proves to be both efficient and rapid. The negatively charged tiopronin/ethidium MPC exhibits, on the other hand, quite slow intercalation kinetics, relative to those of an ethidium cation not attached to an MPC. The kinetics are analyzed as two competing binding interactions. Finally, the tiopronin/ethidium MPC binding to DNA was imaged by atomic force microscopy (AFM).

EXPERIMENTAL SECTION

Chemicals. Ethidium bromide, 3,8-diamino-6-phenylphenanthridine, ethyl chloroformate, trifluoromethanesulfonic anhydride, *N*-(2-mercaptopropionyl)glycine (tiopronin, 99%), sodium borohydride (99%), NaCl (optical grade), and 12-bromo-1-dodecanol (Aldrich) were used as received. All solvents were spectroscopic grade (Fisher or Aldrich); deuterated solvents were obtained from Isotech and Aldrich. $\text{HAuCl}_4 \cdot x\text{H}_2\text{O}$ was synthesized according to the literature,²⁵ as was the *N,N,N*-trimethyl(mercaptoundecyl)-ammonium¹¹ (TMA) ligand. House-distilled water was purified with a Barnstead NANOpure system (>18 M Ω).

Two kinds of DNA were used. DNA with 50–600 base pairs (bp, Roche Diagnostics Corp) was used unless otherwise specified. Gel results showed that the most (by far) abundant strands contained an average of 100 bps. DNA concentration (base pair concentration) is measured by UV absorbance and calculated by following standard protocol. Buffer solutions were prepared according to standard laboratory procedures, and DNA solutions were freshly prepared for fluorescence measurements. For AFM imaging experiments, prehybe DNA (300–1300 bp, most abundant around 600 bp from gel results, Lofstrand Labs) was purified by GFX PCR DNA purification kit (Amersham Pharmacia Biotech) to ensure the absence of proteins or other contaminants that might influence the imaging result. The prehybe DNA was also used in kinetic measurements for comparison and showed no significant difference from the above DNA material in its binding kinetics.

Synthesis of 3,8-Diamino-5-mercaptododecyl-6-phenylphenanthridinium Bromide. The reaction scheme is detailed in Supporting Information. 12-Bromododecyl triflate (**1**) was prepared according to a modified literature¹³ procedure. 3,8-Bis-(ethoxycarbonylamino)-6-phenylphenanthridine (**2**) was prepared in a modified procedure described by Watkins.²⁶ 3,8-Bis-(ethoxycarbonylamino)-6-phenyl-5-(12-bromododecyl)phenanthridine (**3**) was prepared by alkylation of **2** with **1**.¹³ 3,8-Bis-(ethoxycarbonylamino)-6-phenyl-5-(12-thioacetyldodecyl)phenanthridine (**4**) was prepared according to Wolf and Fox.²⁷ Compound **4** was deprotected and hydrolyzed in HBr aqueous solution to prepare 3,8-

- (14) (a) Mirkin, C. A.; Letsinger, R. L.; Mucic, R. C.; Storhoff, J. J. *Nature* **1996**, *382*, 607. (b) Elghanian, R.; Storhoff, J. J.; Mucic, R. C.; Letsinger, R. L.; Mirkin, C. A. *Science* **1997**, *277*, 1078. (c) Storhoff, J. J.; Elghanian, R.; Mucic, R. C.; Mirkin, C. A.; Letsinger, R. L. *J. Am. Chem. Soc.* **1998**, *120*, 1959. (d) Taton, T. A.; Mucic, R. C.; Mirkin, C. A.; Letsinger, R. L. *J. Am. Chem. Soc.* **2000**, *122*, 6305. (e) Park, So-Jung; Lazarides, A. A.; Mirkin, C. A.; Letsinger, R. L. *Angew. Chem., Int. Ed.* **2001**, *40*, 2909.
- (15) (a) Alivisatos, A. P.; Johnson, K. P.; Peng, X.; Wilson, T. E.; Loweth, C. J.; Bruchez, M. P.; Schultz, P. G. *Nature* **1996**, *382*, 609. (b) Loweth, C. J.; Caldwell, W. B.; Peng, X.; Alivisatos, A. P.; Schultz, P. G. *Angew. Chem., Int. Ed. Engl.* **1999**, *38*, 1808.
- (16) McIntosh, C. M.; Esposito, E. A.; Boal, A. K.; Simard, J. M.; Martin, C. T.; Rotello, V. M. *J. Am. Chem. Soc.* **2001**, *123*, 7626.
- (17) Desfrancois, C.; Carles, S.; Schermann, J. P. *Chem. Rev.* **2000**, *100*, 3943.
- (18) Turro, N. J.; Barton, J. K.; Tomalia, D. A. *Acc. Chem. Res.* **1991**, *24*, 332.
- (19) Lerman, L. S. *J. Mol. Biol.* **1961**, *3*, 18.
- (20) (a) Waring, M. J. *J. Mol. Biol.* **1965**, *13*, 269. (b) LePecq, J. B.; Paoletti, C. *J. Mol. Biol.* **1967**, *27*, 87.
- (21) Morgan, A. R.; Lee, J. S.; Pulleyblank, D. E.; Murray, N. L.; Evans, D. H. *Nucleic Acids Res.* **1979**, *7*, 547.
- (22) (a) Bresloff, J. L.; Crothers, D. M. *J. Mol. Biol.* **1975**, *95*, 103. (b) Mandal, C.; Englander, S. W.; Kallenbach, N. R. *Biochemistry* **1980**, *19*, 5819. (c) Macgregor, R. B.; Clegg, R. M. Jr.; Jovin, T. M. *Biochemistry* **1985**, *24*, 5503. (d) Macgregor, R. B.; Clegg, R. M. Jr.; Jovin, T. M. *Biochemistry* **1987**, *26*, 4008.
- (23) Meyer-Almes, F. J.; Porschke, D. *Biochemistry* **1993**, *32*, 4346.

(24) Aguila, A.; Murray, R. W. *Langmuir* **2000**, *16*, 5949.

(25) 25. Brauer, G. *Handbook of Preparative Inorganic Chemistry*; Academic Press: New York, 1965; p 1054.

(26) (a) Watkins, T. I. *J. Chem. Soc.* **1947**, 67. (b) Watkins, T. I. *J. Chem. Soc.* **1952**, 3059. (c) Watkins, T. I. *J. Chem. Soc.* **1958**, 1443.

(27) Wolf, M. O.; Fox, M. A. *Langmuir* **1996**, *12*, 955.

diamino-5-mercaptododecyl-6-phenylphenanthridinium bromide (5).¹³ The final product is a red solid. ¹H NMR (CD₃OD): δ 8.42 (2 H), 7.65 (3 H), 7.65 (3 H), 7.27 (2 H), 6.30 (1 H), 4.38 (2 H), 2.55 (2 H), 1.77 (2 H), 1.51 (2 H), 1.26 (2 H), 1.22–0.95 (14 H) ppm. HRMS (FAB+) of C₃₁H₄₀BrN₃S: calculated 486.2943 for C₃₁H₄₀N₃S⁺, found 486.4027. (more details in Supporting Information)

MPC Synthesis and Ethidium Place Exchange. Tiopronin MPCs were prepared according to Templeton et al.,⁵ and TMA MPCs as described by Cliffl et al.⁸ In both cases, a 3:1 mole ratio of the thiol to AuCl₄[−] was used. TEM results were in agreement with previous reports:^{5,8} average Au core sizes of these nanoparticles are 1.8 and 4.4 nm, respectively, and the average compositions are Au₂₀₁(tiopronin)₈₅ and Au₃₀₀₀(TMA)₉₁₀.

Place exchange of the MPCs with ethidium thiol was carried out in a 3:1 CH₃OH/H₂O solvent mixture. Solutions of ethidium thiol in methanol and of tiopronin or TMA MPCs in H₂O were mixed together; the mixture contained a 1:10 mole ratio of ethidium thiol to thiolate ligands on the MPCs. After the solution was stirred for 2 days, the solvent was removed under vacuum and the solid residue redissolved in water and dialyzed 3–5 days. The mixed-monolayer MPC composition was measured with proton NMR as previously described.⁶ From the ratio of the area of the ethidium aromatic proton peaks around δ = 7–9 to that of either tiopronin or TMA ligands with chemical shifts around δ = 3–4, it was determined that on average a single ethidium thiol was place exchanged onto each MPC. (The NMR spectrum is listed in Supplementary Information.) Statistically this means that a few of the MPCs will have two ethidiums and some none.

Measurements. Fluorescence spectra were taken on an ISA Instruments Jobin Yvon-Spex Fluorolog-3 spectrometer. The cuvette holder was thermostated. Quartz cuvettes were cleaned thoroughly following procedures described before.²⁴ UV–visible spectra were collected on an ATI Unicam UV4 spectrometer. NMR spectra of MPC solutions were obtained with a Bruker AMX 200-MHz spectrometer, using a line-broadening factor of 1 Hz to improve S/N ratio. Reactions were monitored during ethidium thiol synthesis by thin-layer chromatography on 0.25-mm Merck silica gel plates (60F-254). Baxter silica gel 60 Å (230–400 mesh ASTM) was used for flash column chromatography. High-resolution mass spectra were recorded on a VG ZAB-E4F instrument using FAB ionization.

AFM images were taken in air at ambient humidity using a Nanoscope III (Digital Instruments, Santa Barbara, CA) microscope in tapping mode. Nanosensor Pointprobe noncontact/tapping mode silicon probes (Molecular Imaging Corp., Phoenix, AZ) with spring constants of ~50 N/m and resonance frequencies of ~170 kHz were employed. In a typical imaging experiment, the DNA and tiopronin/ethidium MPC complex was ascertained with fluorescence spectra to have formed (normally after 2-h incubation). The DNA concentration was prepared to be 4×10^{-4} M (in base pair concentration) and the MPC concentration 50 times less. Then the solution was diluted ~200 times with 0.1 M MgCl₂ solution to obtain submonolayer surface coverage upon casting droplets of the diluted solution onto freshly cleaved mica (Spruce Pine Mica Co., Spruce Pine, NC). After an incubation of ~1 min, the mica disk was washed with ~1 mL of HPLC grade water and dried in a stream of N₂ for imaging.

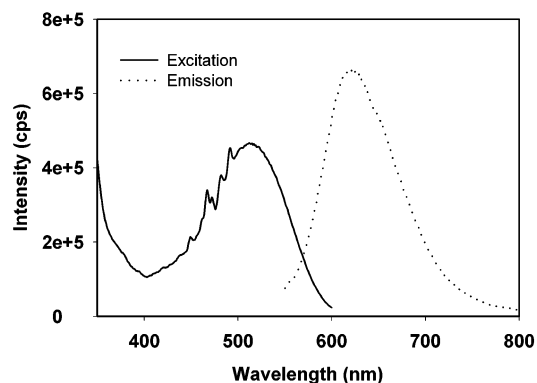


Figure 2. Fluorescence excitation and emission spectra of 3,8-diamino-5-mercaptododecyl-6-phenylphenanthridinium bromide (10^{-4} mol/L in methanol).

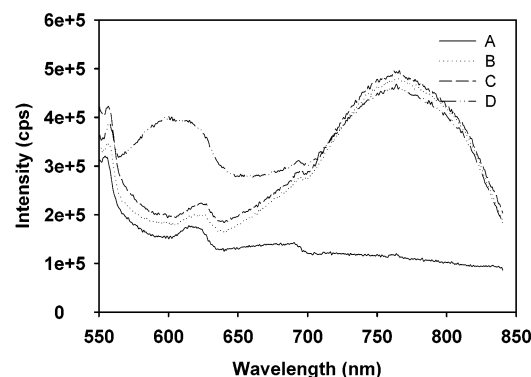


Figure 3. Fluorescence spectra in aqueous tris buffer, pH 8; $\lambda_{\text{EXC}} = 510$ nm. From bottom to top, curve A, DNA alone; this spectrum is similar to the background water spectrum; curve B, tiopronin/ethidium MPC alone; curve C, tiopronin/ethidium MPC with DNA; curve D, tiopronin/ethidium MPC with DNA and 0.1 M NaCl. The DNA base pair and MPC concentrations are about 600 and 2 μ M, respectively. The fluorescence maximum at 760 nm is due to luminescence of the tiopronin MPC itself.

RESULTS AND DISCUSSION

Fluorescence of 3,8-Diamino-5-mercaptododecyl-6-phenylphenanthridinium Bromide (Ethidium Thiol). The aqueous solubility of ethidium thiol (unattached to MPC) is limited, so its absorbance and fluorescence spectra were measured in methanol. The ethidium thiol showed an absorbance maximum at 520 nm, which overlaps the MPC surface plasmon band at the same wavelength. Excitation and emission fluorescence spectra of ethidium thiol (Figure 2) show maximums in excitation at 510 nm and emission at 618 nm, respectively. These spectral properties are very close to those of the underivatized fluorescence center (ethidium bromide), which are λ_{ABS} at 520 nm and λ_{EM} at 600 nm.

Fluorescence of Ethidium Thiolates Attached to MPCs. For both tiopronin/ethidium and TMA/ethidium MPCs, over the concentration ranges employed in the experiments with DNA, ethidium fluorescence near 600 nm was not readily evident above the pH 8 (or at pH 1) tris buffer background (Figure 3, curve A). Compared to the fluorescence intensity of a free ethidium bromide (not attached to MPC) solution of the same concentration, the luminescence of the MPC-attached ethidium center (the 6-phenylphenanthridinium ring) has been quenched completely. In contrast, when free ethidium is simply mixed in solution with a TMA MPC, its fluorescence is reduced by about 80–90% but is still easily measured.

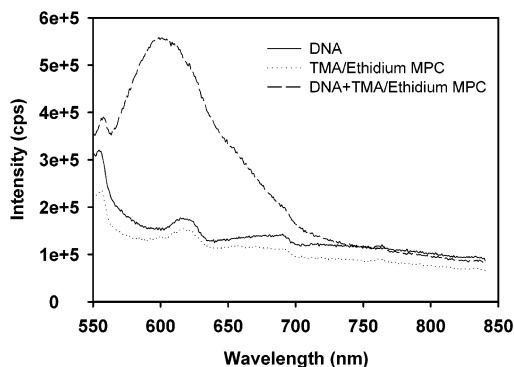


Figure 4. Fluorescence spectra of DNA alone, TMA/ethidium MPC alone, and a mixture of DNA and TMA/ethidium MPC, from top to bottom. The DNA base pair and MPC concentrations are about 600 and 2 μM , respectively.

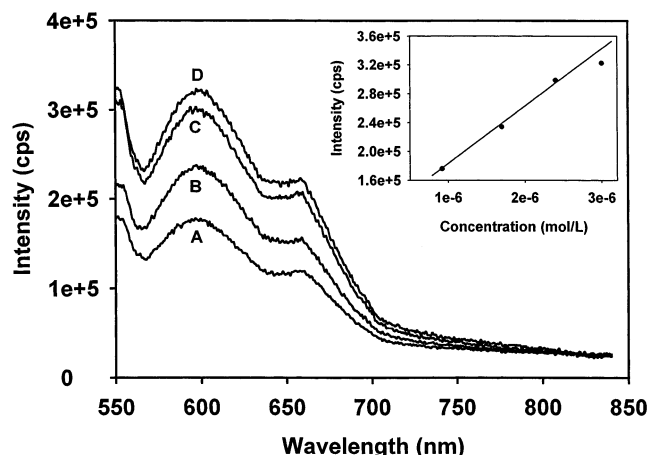


Figure 5. Effect of concentration of added TMA/ethidium MPC on ethidium fluorescence in the presence of DNA. Curves A–D refer to addition of 20, 40, 60, and 80 μL of 12 μM TMA/ethidium MPC into 240 μL of DNA solution (bp concentration 1.1×10^{-3} M). The inset is fluorescence intensity versus MPC concentration.

The large fluorescence maximum in Figure 3B at 760 nm is due to luminescence of the tiopronin MPC itself.⁷ The fluorescence at 760 nm is the same as that of the tiopronin MPC itself, prior to ethidium place exchange, and seems not affected by ethidium interaction with DNA. The tiopronin fluorescence intensity usefully serves as a reference in the following measurements.

We interpret the absence of ethidium fluorescence when attached to the MPCs as efficient energy-transfer quenching of its excited state. From a previous study²⁴ where a dansyl fluorophore was attached to Au MPCs, we know that quenching varies with chain lengths of the fluorophore linker and of the surrounding monolayer and with the loading of fluorophore per MPC. In the case of the tiopronin/ethidium MPC, the surrounding monolayer's chain length is both short and, being quite polar, lacking of hydrophobic interaction structural organization that would restrain motions of the ethidium moiety or its linker chain. Thermal fluctuations consequently bring the ethidium center close to the metal-like Au core and its high density of electronic states. Additionally, the ethidium site gains proximity to the Au core by interaction with the tiopronin monolayer, either electrostatically at higher pH (where the tiopronin carboxylic acids are ionized and the monolayer negative) or at any pH by hydrogen bonding (through the ethidium amine sites). The efficiency of energy-

transfer quenching by MPC nanoparticle cores is, finally, illustrated by the TMA MPC. Although the longer hydrophobic linker in the monolayer of the TMA MPC (Figure 1) and the electrostatic repulsion between it and the cationic ethidium ligand should force the fluorophore on average further away from the Au core, essentially complete quenching of ethidium fluorescence is found for TMA/ethidium MPCs.

The efficient quenching of MPC-attached ethidium by the Au core and the appearance of its fluorescence upon intercalation is a favorable feature of using MPC-attached ethidium as a DNA probe.

Binding of DNA and TMA/Ethidium MPCs. TMA/ethidium MPCs alone show no ethidium fluorescence, as noted above. When DNA is added to a solution of TMA/ethidium MPCs, the ethidium fluorescence becomes readily and immediately observable as shown in Figure 4. This fluorescence is unaffected by adding electrolyte, unlike the case of mixtures of DNA and tiopronin/ethidium MPCs (vide infra). The result of Figure 4 shows that, although bearing a very bulky substituent (i.e., the MPC), intercalation of ethidium into the DNA helix is possible. Undoubtedly aiding this interaction is the cationic halo of quaternary ammonium groups surrounding the MPC, which can interact electrostatically with the anionic DNA phosphate backbone.

Figure 5 shows the increase in ethidium fluorescence intensity at 600 nm when increments of TMA/ethidium MPC are added to a solution containing an excess amount of DNA. The intensity increase is proportional to the quantity of added MPCs, which suggest complete binding between DNA and TMA/ethidium MPCs, and a bound nanoparticle/fluorescence proportionality that can be the basis of quantitative kinetic measurements, as done below. Higher added quantities of MPC resulted in precipitation and subsequently a nonlinear change in emission intensity. Since this quantity of TMA/ethidium MPC should be insufficient to saturate the available DNA base pairs, the precipitation probably reflects an electrostatic cross-linking of DNA by the cationic MPCs. Finally, the TMA/ethidium MPC results allow no inferences regarding intercalation in the major versus minor groove direction. The tiopronin/ethidium MPCs, as discussed below, clearly display two binding modes.

Binding of DNA and Tiopronin/Ethidium MPCs. Intercalation of free ethidium into the DNA helix produces as much as a 25-fold fluorescence enhancement.²⁰ The ethidium–DNA binding constant is large;²⁸ at 1.5 mM cacodylate and base pair concentration $C_{\text{DNA,BP}} = 10^{-4}$ M and $C_{\text{ET}} = 10^{-6}$ M, 98.7% of free ethidium is DNA-bound. Many factors such as electrolyte, temperature, and ethidium and DNA concentration influence ethidium intercalation.

For MPC-attached ethidium, the steric bulkiness of the MPC is potentially an additional factor in ethidium binding to DNA, although the results for TMA/ethidium MPC intercalation (above) show that MPC bulkiness does not necessarily prevent intercalation. However, one might imagine that electrostatic repulsion between the DNA phosphate backbone and the negatively charged surface (partly carboxylate at pH 8) of tiopronin/ethidium MPCs might retard or prevent intercalation of ethidium bound to tiopronin MPCs. Indeed, in a mixture of DNA at 10^{-4} M bp concentration and tiopronin/ethidium MPC at a 50-fold smaller

(28) Fromherz, P.; Rieger, B. *J. Am. Chem. Soc.* **1986**, *108*, 5361.

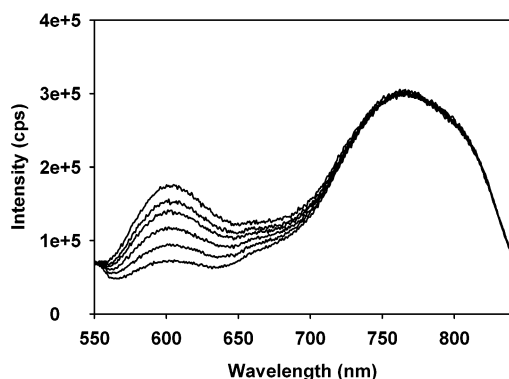


Figure 6. Fluorescence spectra showing the kinetics of the intercalation interaction between $6.6 \mu\text{M}$ tiopronin/ethidium MPCs and $5.3 \times 10^{-3} \text{ M}$ DNA (concentration ratio 1:800). Reaction times from bottom are 5, 12, 30, 60, 90, and 162 min.

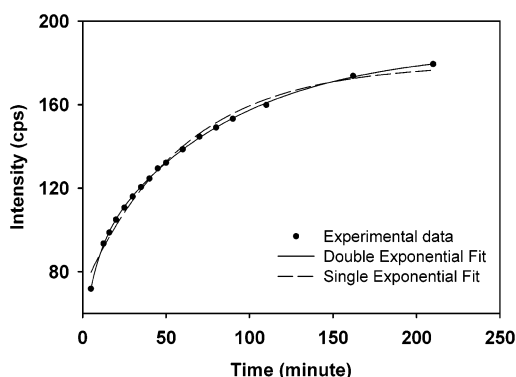


Figure 7. Fits of single- and double-exponential kinetics to experimental fluorescence results (at $\lambda_{\text{EM}} = 610 \text{ nm}$) for intercalation reaction of tiopronin/ethidium at conditions as shown in Figure 6.

concentration, but with no added electrolyte (other than the buffer), intercalation does not occur; no ethidium fluorescence can be detected as shown in Figure 3, curve C. That is, tiopronin/ethidium MPCs and DNA do not bind in 20 mM tris-HCl buffer solutions.

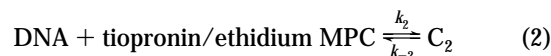
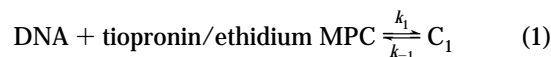
Adding indifferent electrolyte to the preceding solutions provides screening of the DNA and tiopronin/ethidium MPC charges, so that, as shown in Figure 3, curve D, addition of 0.1 M NaCl brings out ethidium emission to be detected at $\sim 600 \text{ nm}$. A minimum of 10^{-2} M NaCl concentration is required in order to resolve a detectable ethidium peak above the similar features of curves A–C (from comparison of software fitted Gaussian peaks).

The reaction of tiopronin/ethidium MPCs with DNA is quite slow. In contrast to the immediate appearance of ethidium fluorescence when DNA and TMA/ethidium MPC solutions were mixed (Figure 4), the growth of the ethidium fluorescence seen in Figure 3, curve D was palpably slow, increasing gradually for hours. Figure 6 shows fluorescence spectra observed during the slow reaction between DNA and tiopronin/ethidium MPCs at a mole ratio of 800:1 (DNA base pair to ethidium). The fluorescence intensity of the tiopronin MPC itself (at 760 nm) remains constant while that of ethidium (at $\sim 600 \text{ nm}$) increases gradually on an hours-long time scale.

The time course of increase in ethidium fluorescence intensity is shown in Figure 7. The increase is rapid in the beginning and then slows. Treating the fluorescence changes as parallel first-order reactions, two exponentials were required to fit the data

(Figure 7). A plot of the logarithm of fluorescence intensity versus time (not shown) showed two straight line segments, consistent with a two-exponential fit. The results in Figure 7 are consistent with Porschke's discussion²³ that two DNA–ethidium complexes, C_1 and C_2 , are formed in two different, parallel intercalation processes. In the present case, these reactions take place on *much* slower time scales than observed²¹ with free ethidium, where the rate constants for intercalation are in the range of 10^5 – $10^6 \text{ M}^{-1} \text{ s}^{-1}$.

Our analysis of Figure 7 assumes parallel reaction pathways (reactions 1 and 2), and a rate law pseudo first order in DNA



(since the concentration of DNA base pairs greatly exceeds that of MPC-attached ethidium). The fluorescence in all experiments was monitored over hours until there was no further increase. In the final equilibrium, essentially all of the MPC-attached ethidium species eventually become intercalated, as determined by comparing the final ethidium fluorescence over a range of DNA concentrations (50–800 excesses of DNA base pairs to MPC-attached ethidium). Using the fluorescence of the MPC itself (Figure 6) as an internal reference, at 298 K the ratio of final ethidium fluorescence and MPC fluorescence intensities was 0.52 – 0.59 for all experiments. Finally, the rapid interconversion of the two forms of ethidium–DNA complexes reported²³ for intercalation of free ethidium with DNA was neglected in our analysis. It is unclear that the analysis could resolve it, and interconversion by ethidium migration within the DNA base pair structure should be difficult given the bulky MPC attached to the intercalated ethidium.

Table 1 shows the results of analysis of data for multiple experiments ($n \geq 2$, including different preparations of tiopronin/ethidium MPCs) using rate law expressions derived for parallel reactions using conventional kinetic theory. The low value of DNA concentration meant that results for the back reaction rate constants k_{-1} and k_{-2} are more reliable than the forward reaction values, whose values were estimated as being nearly identical. The equilibrium constants for reactions 1 and 2 are ~ 40 and ~ 300 , respectively, at 298 K . In the Porschke kinetic study²³ on free ethidium binding, the binding constants for major versus minor groove differed by 10-fold. The MPC-attached ethidium binding equilibrium constants differ by a similar (8-fold) factor.

Experiments at two modestly different temperatures (Table 1) give a rough estimation of the activation energy for tiopronin/ethidium MPC binding with DNA. The activation energy barrier for the off-reaction of reaction 1, k_{-1} , was estimated as $\sim 15 \text{ kJ/mol}$. Although this is a very crude measurement, this parameter is quite small compared with the results²³ for free ethidium. The small off-reaction barrier is consistent with the slowness of the MPC-attached ethidium reaction.

We turn next to the question of why the reaction between DNA and tiopronin/ethidium MPCs is so slow. Possible factors are (a) the steric bulk of the MPC appendage borne by the intercalating ethidium, (b) electrostatic depression of the concentration of

Table 1. Rate Constants for Tiopronin/Ethidium MPC Intercalation with DNA^a

<i>T</i> (K)	<i>k</i> ₁ (M ⁻¹ s ⁻¹)	<i>k</i> ₂ (M ⁻¹ s ⁻¹)	<i>k</i> ₋₁ (s ⁻¹)	<i>k</i> ₋₂ (s ⁻¹)
278.6	$(5 \pm 2) \times 10^{-2}$	$(2 \pm 2) \times 10^{-2}$	$(1.2 \pm 0.05) \times 10^{-3}$	$(1.5 \pm 0.2) \times 10^{-4}$
298.0	$(7 \pm 4) \times 10^{-2}$	$(3 \pm 2) \times 10^{-2}$	$(1.9 \pm 0.05) \times 10^{-3}$	$(1.0 \pm 0.2) \times 10^{-4}$

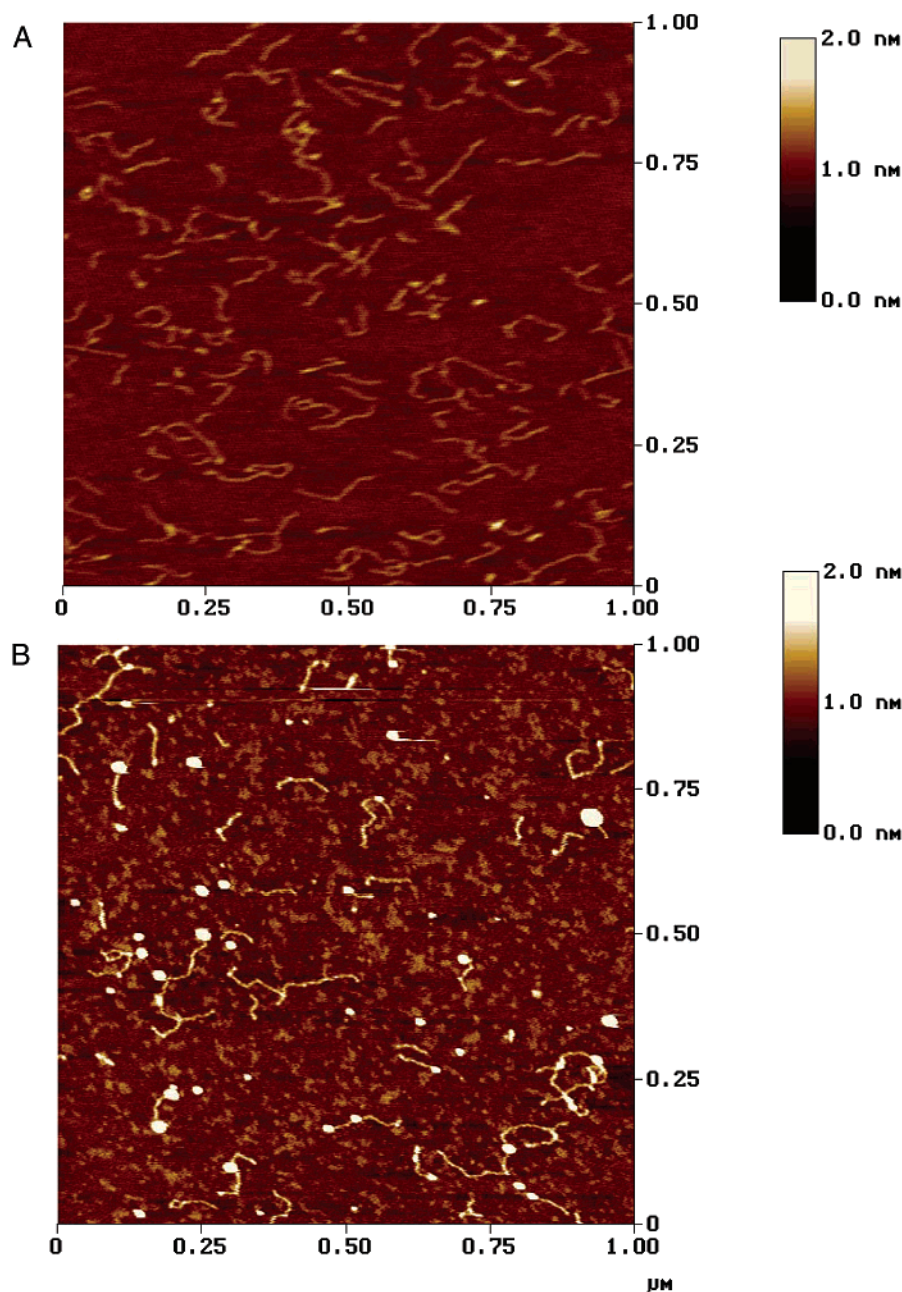
^a Data analysis is detailed in Supporting Information.

Figure 8. AFM image of (A) DNA alone and (B) DNA complex with tiopronin/ethidium MPC.

negatively charged tiopronin/ethidium MPCs caused by the ionic space charge around the negatively charged DNA, and (c) decreased intercalative reactivity of the ethidium cation toward DNA caused by ethidium electrostatic and/or hydrogen-bonding attraction to the outer shell of the MPC monolayer.

In regard to possible steric effects, we point to the fast reaction kinetics of the TMA/ethidium MPCs described above. The TMA MPCs are even larger (in core size) than the tiopronin MPCs. So

while it is not possible to say that steric restraints on the tiopronin/ethidium MPC binding reaction to DNA are unimportant, it is hard to argue that they are a dominant factor in slowing the binding reaction kinetics.

In regard to ionic space charge effects, where the concentration of MPCs around the DNA is electrostatically depressed, we refer to Schellman,²⁹ who reported on the electrical double layer and zeta potential of double-stranded DNA. Modeling DNA as a

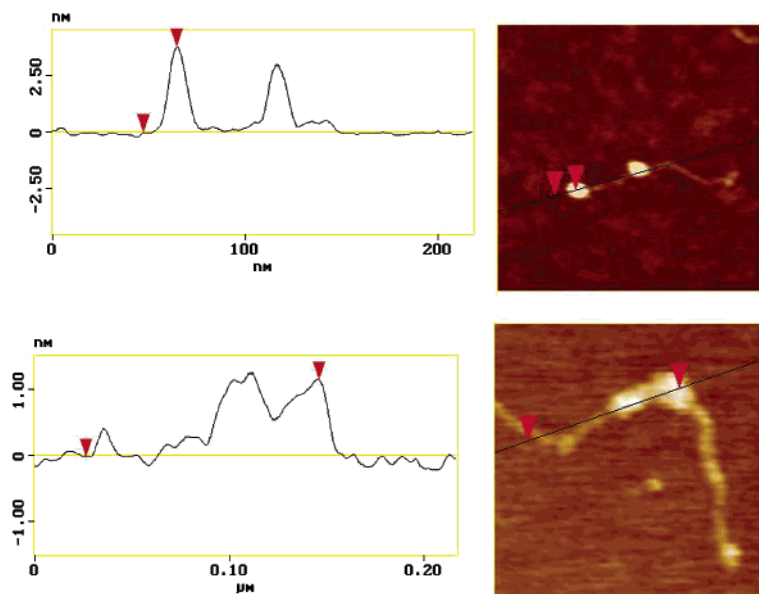


Figure 9. Section plot of DNA complexed with tiopronin/ethidium MPC.

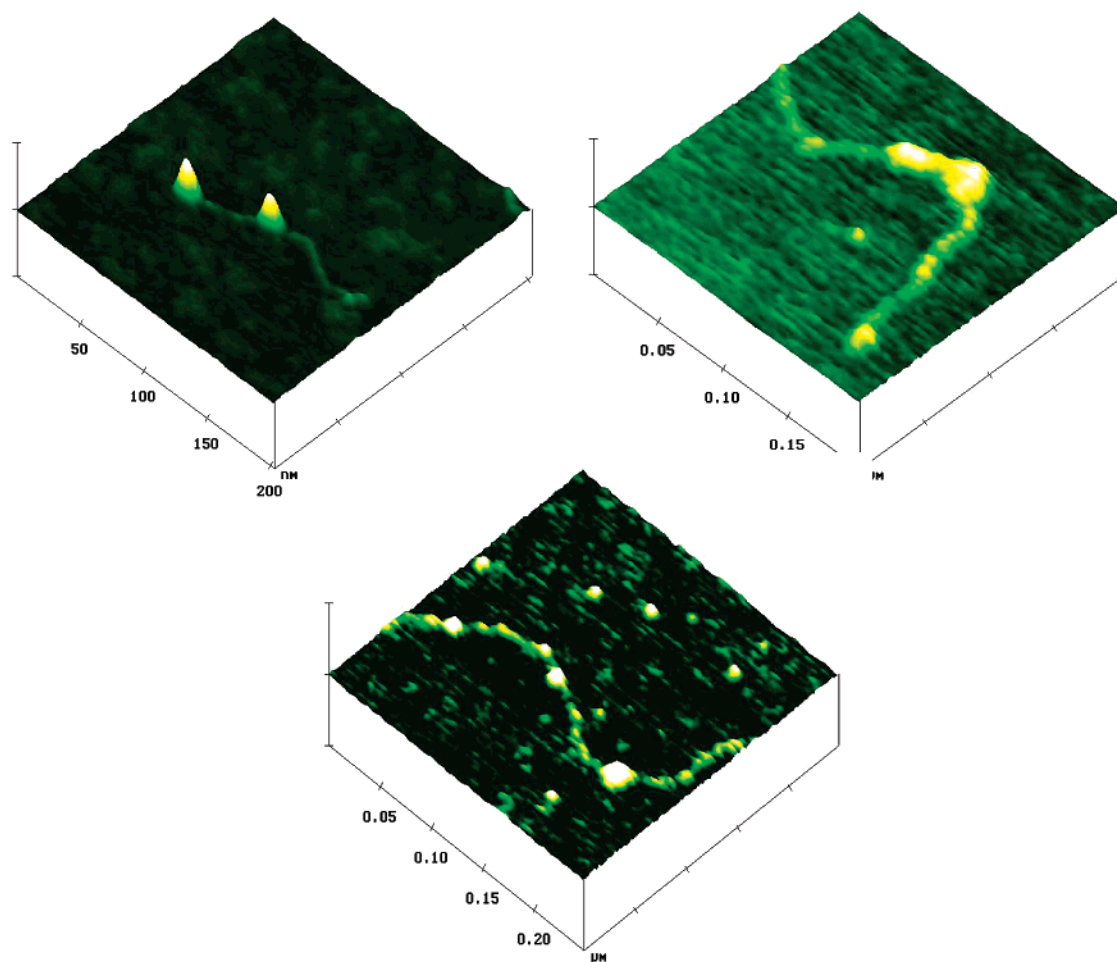


Figure 10. Surface plots of DNA complexed with tiopronin/ethidium MPC.

uniformly charged cylinder, the Stern layer thickness was estimated as 0.6 nm relative to the cylinder's central axis. We will assume that intercalation can take place once the ethidium reaches DNA Stern layer distance. Based on $Y_0 = 2.6$ ($Y_0 = e\xi/kT$) (ξ is the potential at the Stern layer), using double-layer theory³⁰ and considering the 0.1 M NaCl concentration, one can estimate the

MPC concentration as a function of distance from the DNA stern layer. The electrolyte should screen tiopronin carboxylate charges (of which there is a large number, given the nanoparticle composition $Au_{201}(tiopronin)_{85}$) remote from the (lone) ethidium site and only those immediately around that site should have importance in electrostatic repulsion of the MPC; for simplicity,

we assume that these offer a charge equivalent to a univalent anion. Two scenarios are then considered. In one, the 1.6-nm-long⁸ ethidium linker chain is fully extended, which would place the ethidium 0.9 nm outward from the 0.7-nm-long⁶ tiopronin sites. The double-layer calculation in this case shows that the MPC concentration 0.9 nm away from the DNA Stern layer is 36% of its bulk concentration. In the second scenario, the ethidium is assumed to lie in the same plane as the uninegative tiopronin charge, in which case the MPC concentration is 7% of the bulk concentration. These rough estimates show that ionic space charge effects are significant but probably not substantial enough to alone cause the slow reaction kinetics.

The final rationale for the slow tiopronin/ethidium MPC binding to DNA rests on the ethidium moiety's interaction within its own MPC monolayer—which as mentioned above can be electrostatic or hydrogen bonding in nature. If the free energies of these interactions rival that of the ethidium/DNA intercalation, then both the net equilibrium constant and kinetics for ethidium intercalation would be depressed, as is observed. Although the available information does not allow a quantitative estimation of the competing energetics, we presume that this is the major operative effect. This conclusion is entirely consistent with the high reactivity of the TMA/ethidium MPCs with DNA, where the energetics of intercalation of the ethidium cation would, if anything, be enhanced by its repulsion from the cationic TMA monolayer.

AFM Imaging. AFM has been an important tool for study of DNA structures and DNA–protein interactions since its invention.³¹ In this report, AFM provides further direct evidence of binding of tiopronin/ethidium MPCs to DNA. Figure 8A is an image of surface-deposited prehybe DNA; Figure 8B shows a similar image but for prehybe DNA that had been incubated with tiopronin/ethidium MPCs for 2 h before surface depositing. The bright dots in (B) represent MPCs. (The sample was thoroughly

rinsed with water to remove any microcrystallites.) An image (not shown) prepared from much more dilute solution of the tiopronin/ethidium MPC–DNA complex also showed bright dots coincident with DNA chains. In both sets of images, a large fraction of the MPC bright dots were coincident with DNA chains; Figure 9 and Figure 10 show an enlarged view that reinforces this observation. Qualitatively, it seems that many of the MPC images are coincident with the ends of the DNA chains. Not all of the MPC images are coincident with the DNA chains, which is not surprising since (a) the incubation time was less than that shown in Figure 6 to reach complete equilibrium binding and (b) statistical aspects of the place exchange reaction, for which the *average* was one ethidium thiolate per MPC, say that some MPCs will bear no ethidium sites.

The apparent diameter of the MPCs in the AFM image is greater than those known^{5,8} from transmission electron microscopy results, because of the image convolution with the tip diameter. Line scans more accurately illustrate the MPC dimension, as shown in Figure 9. The height of the DNA image is ~0.4 nm and that of the MPC above it ranged from 1 to 4 nm, mostly toward the larger of that range. The apparent heights of the two MPCs each in Figure 9 sections 1 and 2 are 3.3 and 2.8 nm and 1.2 and 1.3 nm, respectively. The dispersity in MPC dimensions is consistent with that known⁵ from previous TEM images. Surface plots shown in Figure 10 provide a 3-D view of the DNA–MPC complex.

ACKNOWLEDGMENT

This work was supported by a grant from the National Science Foundation. The assistance of Professor Dorothy Erie and Hong Wang (UNC-CH) in AFM experiments is gratefully acknowledged.

SUPPORTING INFORMATION AVAILABLE

Additional information as noted in text. This material is available free of charge via the Internet at <http://pubs.acs.org>.

(29) Schellman, J. A. *Biopolymers* **1977**, *16*, 1415.

(30) Bard, A. J.; Faulkner, L. R. *Electrochemical Methods. Fundamentals and Applications*; John Wiley & Sons 1980; p 488–548.

(31) Hansma, P. K.; Elings, V. B.; Marti, O.; Bracker, C. E. *Science* **1988**, *242* (4876), 209. (b) Cherny, D. I.; Fourcade, A. F.; Svinarchuk, F.; Nielsen, P. E.; Malvy, C.; Delain, E. *Biophys. J.* **1998**, *74*, 1015.

Received for review May 17, 2002. Accepted July 11, 2002.

AC0257804